A simulation study of an asymmetric exclusion model with open boundaries and random rates

1999 J. Phys. A: Math. Gen. 32 2527

(http://iopscience.iop.org/0305-4470/32/13/005)

J. Phys. A: Math. Gen. **32** (1999) 2527–2540. Printed in the UK PII: S0305-4470(99)99393-9

A simulation study of an asymmetric exclusion model with open boundaries and random rates

M Bengrine†, A Benyousseff†, H Ez-Zahraouy†, J Krug‡, M Loulidi† and F Mhirech†§

† Laboratoire de Magnetisme et de Physique des Hautes Energies, Departement de Physique, Faculté des Sciences, Rabat, Morocco
‡ Fachbereich Physik, Universität GH Essen, D-45117 Essen, Germany

Received 16 November 1998

Abstract. Using numerical simulations, we study the asymmetric exclusion model with open boundaries, particlewise disorder and parallel dynamics. At each time step, particles are injected at the left boundary with probability $\alpha\Delta t$, removed on the right with probability $\beta\Delta t$, and jump in the bulk with probability $p_\mu\Delta t$, where p_μ is a random rate associated with each injected particle μ. The parameter Δt interpolates between fully parallel ($\Delta t = 1$) and random sequential ($\Delta t \to 0$) dynamics. The phase diagram in the (α, β)-plane displays high-density, low-density and maximum-current phases, with the first-order transition line between high- and low-density phases shifted away from the line $\alpha = \beta$. Within the low-density phase a platoon phase transition occurs, many features of which can be explained using exact results for asymmetric exclusion with particlewise disorder on the ring. In a certain region of parameter space the disorder induces a cusp in the current–density relation at maximum flow. Our simulations indicate that this does not affect the topology of the phase diagram, nor the familiar $1/\sqrt{x}$-decay of the density profile in the maximum-current phase.

1. Introduction

Collective transport in single-file systems has a wide range of applications ranging from biopolymerization [1] to highway traffic [2]. Driven single-file systems are exceedingly sensitive to the boundary conditions governing the in- and outflow of particles, to the extent that phase transitions among different bulk states can be induced by a change of boundary rates [3]. By the same token spatially distributed bottlenecks [4–6] or defect particles with slower intrinsic jump rates [7–11] can have dramatic effects, causing macroscopically inhomogeneous density profiles on ever increasing length scales. A classic example combining these features—inflow, outflow and defect particles—is the problem of tunnel traffic with a range of vehicular velocities first analysed by Newell [12].

A great deal of progress has been achieved in past years in our understanding of boundary- and disorder-induced phase transitions in driven single-file systems. Among the highlights, the exact solution of the totally asymmetric exclusion process (TASEP) with open boundaries should be mentioned [13, 14], which was recently extended to the case of parallel update [15, 16], as well as the solution of the TASEP with particlewise disorder and a variety of update procedures by Evans [17]. In contrast, little is known analytically about systems with spatially distributed defects [6].

§ E-mail address: mhirech@fsr.ac.ma

0305-4470/99/132527+14$19.50

In this paper we present the results of an exploratory numerical study of a model which combines, in the spirit of Newell [12], open boundary conditions and random jump rates associated with particles. Specifically, in our model particles jump to the right to vacant nearest neighbour sites with a probability $p_\mu \Delta t$ in each (discrete) time step, where p_μ is a quenched random variable associated with particle μ (its 'intrinsic' jump rate) and $\Delta t \in (0, 1]$ is a model parameter that allows us to interpolate between the cases of fully parallel ($\Delta t = 1$) and random sequential ($\Delta t \to 0$) updates. At the right (left) boundary particles are injected (extracted) with probability $\alpha \Delta t$ ($\beta \Delta t$). A detailed description of the model is provided in section 2.

Our primary objective is to determine the phase diagram of the model in the (α, β)-plane, which is known analytically only in the pure case ($p_\mu \equiv p$ for all μ) [13–16]. As described in section 3.1, the overall topology of the phase diagram corresponds to that of the pure system. Quantitative differences can be understood from the current–density relation of the disordered model with periodic boundary conditions (section 3.2). In the periodic case the particlewise disorder induces a transition into an inhomogeneous low-density phase where 'platoons' (queues) form behind exceptionally slow particles [18]. In sections 3.3 and 3.4 we show that most features of this transition survive in the open system. Section 3.5 addresses the behaviour in a region of parameter space where the density $\rho_{\max}$ of maximum flow coincides with the critical density ρ^* of the platoon phase transition, and some conclusions are given in section 4.

2. Model

We consider a one-dimensional lattice of length L. Each site is either occupied by one particle or is empty. A configuration of the system is characterized by binary variables $\{\tau_i\}$ where $\tau_i = 0$ ($\tau_i = 1$) if site i is empty (full). During a time interval Δt, each particle μ, hops with probability $p_\mu \Delta t$ to its right if this site is empty and does not move otherwise. Particles are injected at the left boundary with a rate $\alpha \Delta t$ and removed on the right with a rate $\beta \Delta t$. During one update step the new particle positions do not influence the rest and only previous positions have to be taken into account. The advantage of parallel update, with respect to sublattice or sequential update is that all sites are equivalent, which should be the case in a realistic model with translational invariance.

Thus, if the system has the configuration $\tau_1(t), \tau_2(t), \ldots, \tau_L(t)$ at time t it will change at time $t + \Delta t$ to the following.

For $1 < i < L$, $\tau_i(t + \Delta t) = 1$ with probability

$$q_i = \tau_i(t) + \tau_{i-1}(t)(1 - \tau_i(t))p_\mu \Delta t - \tau_i(t)(1 - \tau_{i+1}(t))p_\nu \Delta t \tag{1}$$

where p_μ and p_ν denote the jump rates of the particles at sites $i - 1$ and i, respectively, and $\tau_i(t + \Delta t) = 0$ with probability $1 - q_i$.

For $i = 1$, $\tau_1(t + \Delta t) = 1$ with probability

$$q_1 = \tau_1(t) + \alpha \Delta t(1 - \tau_1(t)) - \tau_1(t)(1 - \tau_2(t))p_\nu \Delta t \tag{2}$$

where p_ν denote the jump rate of the particle at site 1, and $\tau_1(t + \Delta t) = 0$ with probability $1 - q_1$.

For $i = L$, $\tau_L(t + \Delta t) = 1$ with probability

$$q_L = \tau_L(t) + \tau_{L-1}(t)(1 - \tau_L(t))p_\mu \Delta t - \beta \Delta t \tau_L(t) \tag{3}$$

where p_μ denotes the jump rate of the particle at site $L-1$, and $\tau_L(t+\Delta t) = 0$ with probability $1 - q_L$.

In the following we shall consider that an intrinsic probability, $p_\mu \in [c, 1]$, is assigned to each particle μ, randomly drawn from the following continuous probability distribution [9]

$$f(p) = \frac{n+1}{(1-c)^{n+1}}(p-c)^n \tag{4}$$

where we will mostly choose $n = 1$ and $c = \frac{1}{2}$; the inhomogenous platoon phase in the periodic system exists at sufficiently low-density provided $n > 0$, see [18] and section 3.3. For each particle that enters the system at $i = 1$ a new jump rate is picked, which the particle then keeps until it exits at $i = L$.

3. Simulation results and discussion

We use lattices of sizes $L = 2000$–10^5 and a random initial distribution of particles. After a sufficiently long period of time, the system reaches a stationary state and we compute the average $\langle w \rangle$ of any parameter w by averaging $w(t)$ ($t = m\Delta t$, m integer) over 2×10^5–10^7 time steps. Note that, in contrast to the case of a periodic lattice [9, 19], a separate disorder average is not necessary, because new particles are constantly injected into the system.

3.1. Phase diagram

The method for numerically determining the phase diagram was described previously for the pure case [20]. Figure 1(*a*) shows the dependence of the bulk density ρ on the rate of injected particles, α, for a large and fixed value of Δt ($\Delta t = 1$, 'fully parallel update') and for several values of the rate of removed particles β. It is clear that for a fixed value of β less than a critical value β_c, the bulk density first increases smoothly when increasing the rate of injected particles α (*low-density phase*), until at a value $\alpha^*(\beta)$ a first-order transition characterized by a jump discontinuity brings the system into the *high-density phase* where the density becomes independent of α. The density jump decreases in magnitude with increasing β, and vanishes at the critical point $\beta = \beta_c$. For β greater than β_c one finds a maximal current phase, where the bulk density and the current are independent on the rate of injected and removed particles. We will see in section 3.2 how the current and density in this phase can be obtained from the analytic solution for the case of periodic boundary conditions [17].

It is worth pointing out that, in general, the dependence of the bulk density on the rate of injected particles α in the low-density phase is nonlinear. This is also true in the pure system with parallel update, where the functional relation $\rho(\alpha)$ is known analytically [15, 16]. Only for the pure system with random sequential update is ρ equal to α [3, 13, 14]. The same statement applies, of course, to the dependence of ρ on β in the high-density phase.

A qualitative difference compared with the pure case is that the first-order transition occurs at a value $\alpha^*(\beta)$ which is slightly smaller than the rate of removed particles β. This is an effect of the disorder in our model, which breaks the particle–hole symmetry that would otherwise guarantee $\alpha^*(\beta) = \beta$ [13–16, 20]. In order to provide more information concerning the coexistence line between the low- and high-density phases we show in figure 1(*b*), for $\Delta t = 1$ and $\beta = 0.1$, the density profile as a function of the position. The data reveal that for $\alpha = \beta$, the density profile does not depend linearly on the position, as would be expected in the presence of particle–hole symmetry. Instead, the density profile becomes linear for $\alpha = \alpha^*$, slightly inferior to the value of removed particles β (here $\beta = 0.1$, $\alpha^* = 0.0995$). The existence of a linear profile at coexistence is the result of a fluctuating shock front which separates the high-density region from the low-density one.

For the purpose of computing the phase diagram we identify the first-order transition by the appearance of a peak in the first derivative of $\rho(\alpha)$ with respect to α, indicative of the (smeared

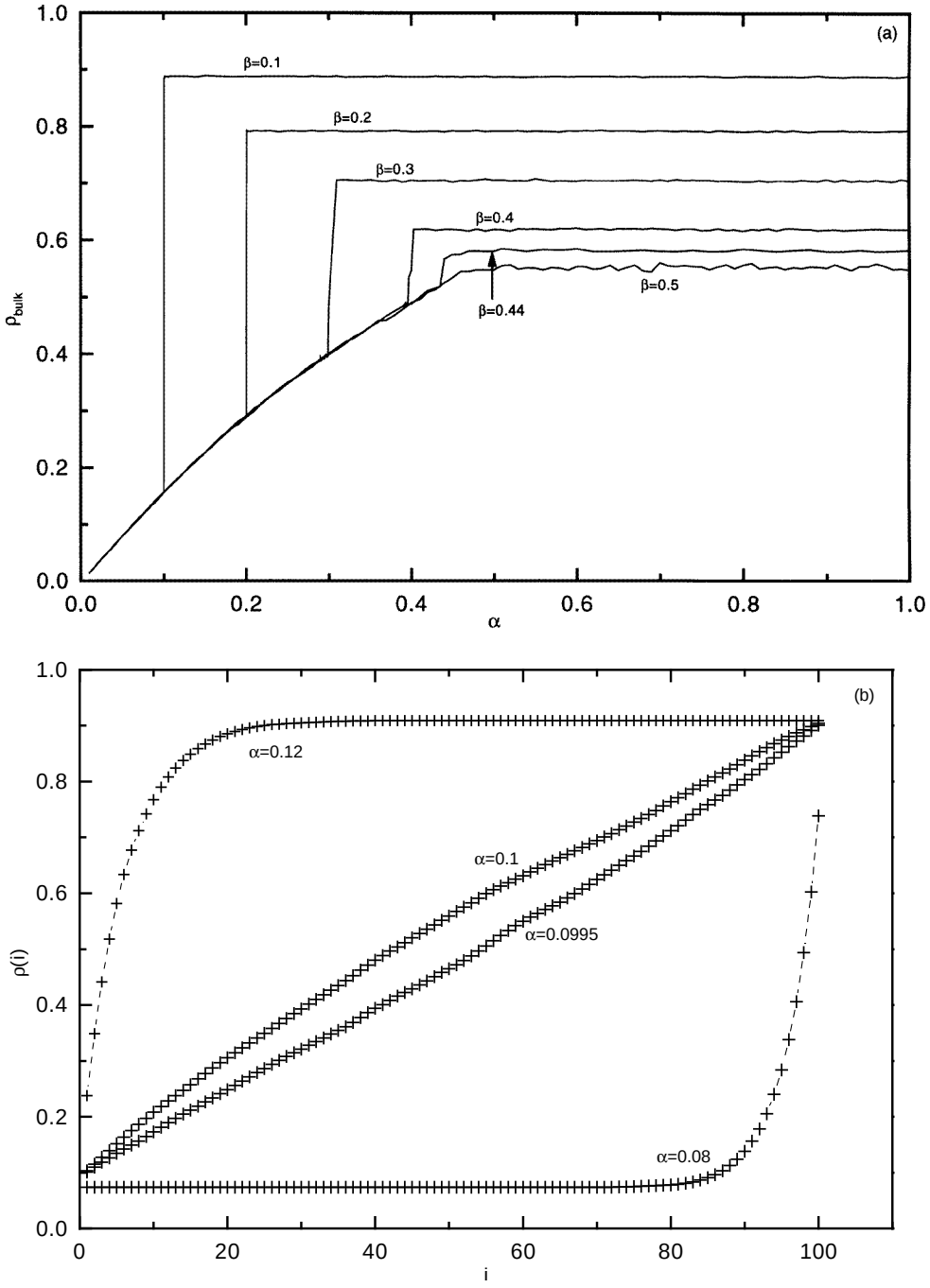

Figure 1. (*a*) The variation of the bulk density versus the rate of injected particles α, for $L = 2000$ and $\Delta t = 1$. (*b*) The density profiles near the first-order transition for $L = 2000$, $\Delta t = 1$ and $\beta = 0.1$.

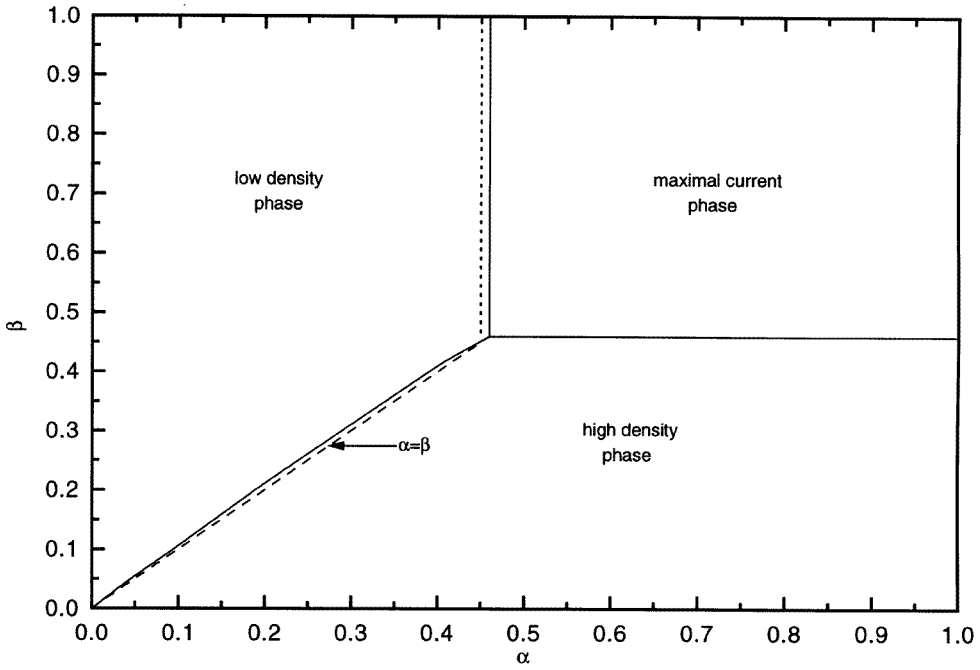

Figure 2. The phase diagram in the (α, β)-plane for $L = 2000$ and for $\Delta t = 1$, $n = 1$ and $c = 0.5$. The vertical dotted line represents the platoon transition ($\rho = \rho^*$) in the low-density phase.

out) discontinuity shown in figure 1. At the second-order transition the peak is replaced by a jump. Collecting these results we obtain the phase diagram as shown in figure 2 for $\Delta t = 1$. The low-density phase, high-density phase and maximal current phase are recovered with the end point (α_c, β_c) such as $\alpha_c = \beta_c = 0.46$. In the case of $\Delta t = 0.1$ (not shown in the figure) we find $\alpha_c = \beta_c = 0.36$. To put these results in perspective, we note that for the *pure* version of our model, i.e. with $p_\mu \equiv p$ for all particles, the exact solution [15, 16] gives the critical value

$$\alpha_c^{\text{pure}}(p, \Delta t) = \frac{1 - \sqrt{1 - p\Delta t}}{\Delta t} \tag{5}$$

which is a monotonically increasing function of p. Since in the disordered case $c \leqslant p_\mu \leqslant 1$, we expect that $\alpha_c^{\text{pure}}(c, \Delta t) \leqslant \alpha_c \leqslant \alpha_c^{\text{pure}}(1, \Delta t)$. For $c = \frac{1}{2}$ this yields $0.293 \leqslant \alpha_c \leqslant 1$ for $\Delta t = 1$, and $0.253 \leqslant \alpha_c \leqslant 0.513$ for $\Delta t = 0.1$, consistent with our numerical estimates. Moreover, since (5) also increases monotonically as a function of Δt for any p, it explains why the maximum-current phase gains more space with decreasing Δt. Note, in particular, that for $\Delta t = 1$ the maximum-current phase exists in our model only due to the random hopping rates; in the absence of disorder, when $p = \Delta t = 1$, it disappears altogether [21], as is most easily understood within the framework of the waiting-time representation [22].

3.2. Current–density relation

The current–density relation for the disordered model can be obtained analytically in the hydrodynamic limit ($L \to \infty$) using the known invariant measure [17] for the particle headways (the number of vacants sites in front of a given particle μ) defined by $u_\mu = x_{\mu+1} - x_\mu - 1$, where x_μ is the position of particle μ. Using the headway distribution, the

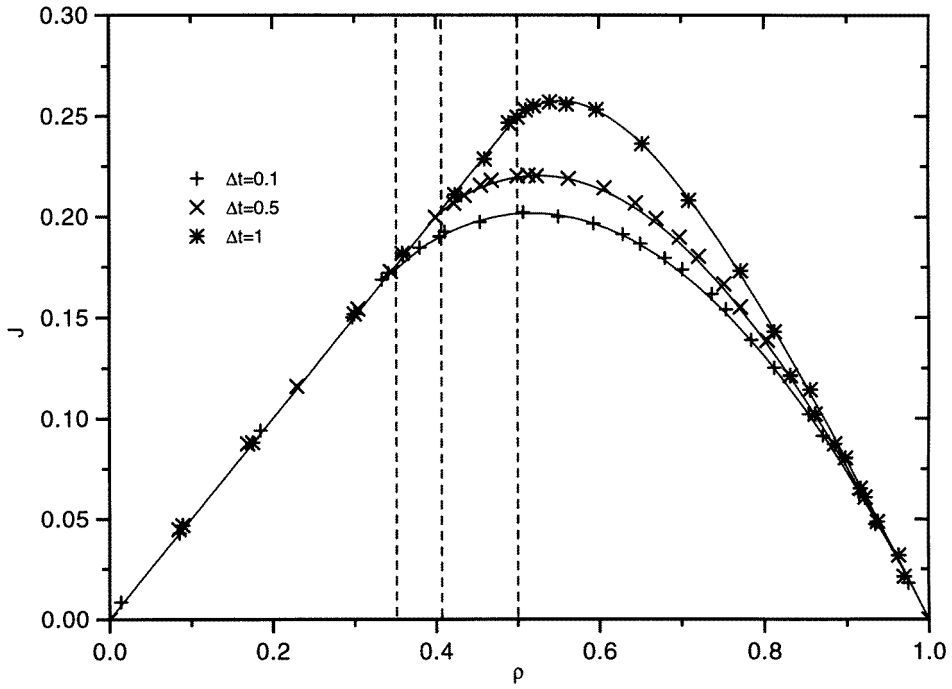

Figure 3. The variation of the current J as a function of density ρ for $L = 2000$, $n = 1$ and $c = \frac{1}{2}$. The vertical dotted lines represent the platoon transition ($\rho = \rho^*$) in the low-density phase for each value of Δt. The symbols represent our simulation data, while the full curves represent the analytical results.

average headway $\langle u_\mu \rangle$ can be computed for each particle. Averaging this with respect to the random rates p_μ, yields an implicit equation for the stationary particle velocity $v(\rho)$, which takes the form

$$\rho = \left[1 + (1 - v\Delta t)v \int_c^1 \frac{f(p)}{(p - v)} \, \mathrm{d}p \right]^{-1}. \tag{6}$$

This relation holds for densities $\rho \in [\rho^*, 1]$, where ρ^* is the critical density for the onset of platoon formation [9, 10, 17, 18]. The value of ρ^* is found by setting $v = c$ in the right-hand side of (6). Using the jump rate distribution (4), this yields

$$\rho^*(n, c, \Delta t) = \frac{n(1 - c)}{n + c - c^2(n + 1)\Delta t}. \tag{7}$$

For ρ less than ρ^*, the overall speed will be set by the slowest particles, and consequently $v = c$.

The current–density relation is then given by $J(\rho) = \rho v(\rho)$, where v is determined from (6) for $\rho > \rho^*$ and $v = c$ for $\rho < \rho^*$; in the low-density regime the current is *linear* in the density. In figure 3, the analytic prediction for the current in the infinite system is compared with simulations of finite open systems. By sampling the different regions of the (α, β)-phase diagram, we collect pairs of values $(\rho, J(\rho))$, which are depicted by the symbols in figure 3. The excellent agreement with the analytic curve shows that the finite open system is well described by its hydrodynamic limit. Figure 4 shows the same kind of comparison for the particle velocity $v(\rho)$.

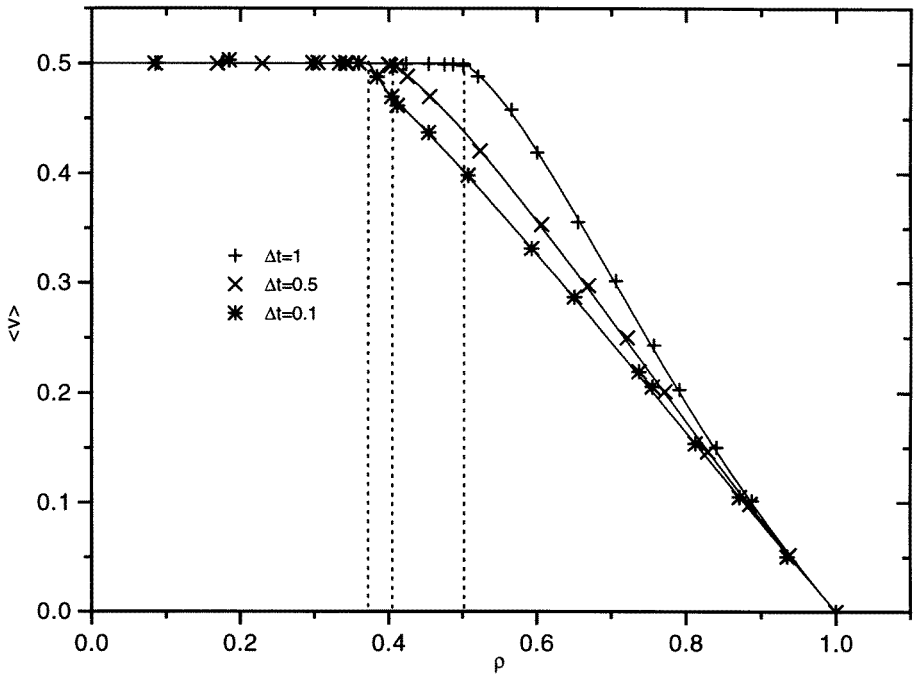

Figure 4. The variation of the velocity $\langle v \rangle$ as a function of density ρ, for $L = 2000$, $n = 1$ and $c = \frac{1}{2}$. The vertical dotted lines represent the platoon transitions in the low-density phase for $\Delta t = 1$, $\Delta t = 0.5$ and $\Delta t = 0.1$. The symbols represent our simulations results, while the full curves represent the analytic results.

Of particular interest is the maximal current $J_{\max}$ and the corresponding density $\rho_{\max}$, since this is the density selected in the maximal current phase [3]. We find that both quantities increase with increasing Δt. For instance, $(J_{\max}, \rho_{\max}) \approx (0.2016, 0.5175)$ for $\Delta t = 0.1$, $(J_{\max}, \rho_{\max}) \approx (0.2203, 0.5250)$ for $\Delta t = 0.5$ and $(J_{\max}, \rho_{\max}) \approx (0.2576, 0.5516)$ for $\Delta t = 1$. Note that in the absence of randomness particle-hole symmetry enforces that $\rho_{\max} = \frac{1}{2}$ independent of Δt.

3.3. The platoon phase

In the presence of random jump rates associated with the particles the infinite system displays a phase transition at $\rho = \rho^*$ [8–10, 17]. Through a mechanism closely related to Bose–Einstein-condensation [10], the stationary distribution of particle headways ceases to be normalizable below ρ^*, and consequently the stationary density profile on a finite ring phase separates into a region of density ρ^* and a macroscopic gap (the 'condensate') of density zero. Numerically, the transition can therefore be be located by monitoring the variance of the headways [9]

$$\Delta^2 = \langle \langle u_\mu^2 \rangle_\mu - \langle u_\mu \rangle_\mu^2 \rangle \tag{8}$$

where $\langle\,\rangle_\mu$ means the average over all the values of the gap, as a function of density and system size. For $\rho > \rho^*$, Δ^2 is independent of system size, while for $\rho < \rho^*$ it is dominated by the macroscopic gaps and acquires an L-dependence.

In figure 5 we show $\Delta^2(\rho)$ for the open system with $\Delta t = 0.1$ and for two values of the system size $L = 2000$ and $L = 500$. As expected, the data for the two system sizes coincide for $\rho > \rho^*$ but differ for $\rho < \rho^*$. It is worth noting, however, that the L-dependence in the

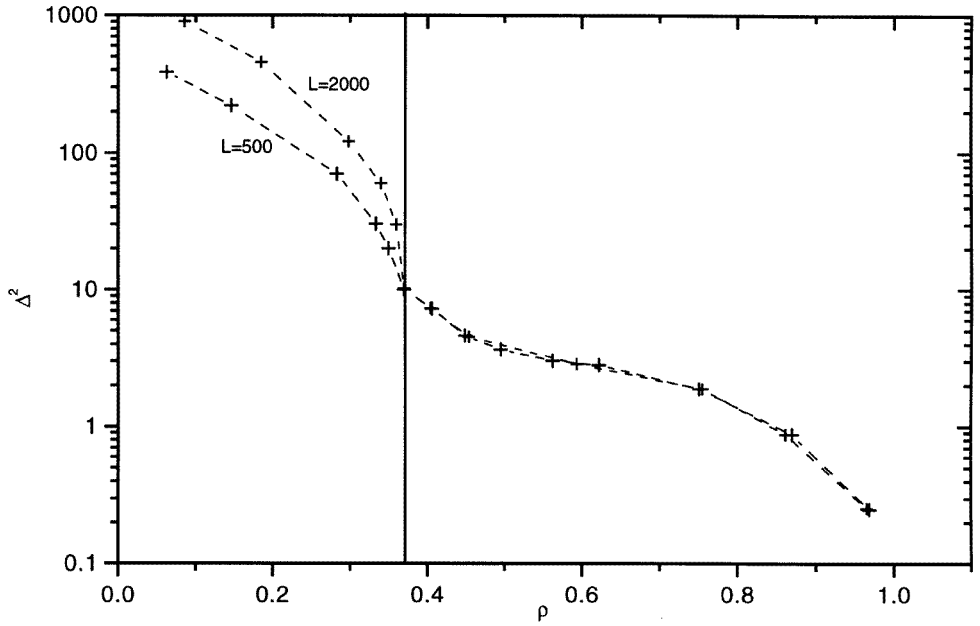

Figure 5. The semilogarithmic plot of the variance of headways Δ^2 versus density ρ for $\Delta t = 0.1$, $n = 1$ and $c = \frac{1}{2}$. The vertical full line represents the platoon transition ($\rho = \rho^*$).

low-density phase is much weaker than for the periodic system, where it can be shown [9] that, assuming complete phase separation in the stationary state,

$$\Delta^2 \approx (L/\rho)(1 - \rho/\rho^*)^2. \tag{9}$$

In the open system this limit is never reached, because the gaps can only grow for a time $T \sim L$ of the order of the residence time of particles in the system. Since the large gaps between platoons grow only sublinearly in time (see below), they always remain small compared with L.

To illustrate the effect of Δt we show in figure 6 the variation of ρ^* as a function of Δt. The points show numerical data obtained through measurements of $\Delta^2(\rho)$, as illustrated in figure 5, while the full curve show the prediction (7), which for $n = 1$, $c = \frac{1}{2}$ reduces to

$$\rho^*(\Delta t) = \frac{1}{3 - \Delta t}. \tag{10}$$

The increase of ρ^* with increasing Δt can be interpreted [18] in terms of a competition between two distinct kinds of randomness: the (static) disorder in the jump rates and the (dynamic) stochasticity in the updating. In the low-density phase, the disorder in the jump rates dominates. By increasing Δt the dynamic stochasticity is reduced and therefore the influence of the static disorder grows, leading to an expansion of the low-density phase. The location of the platoon phase transition in the (α, β)-phase diagram is shown by a dotted line in figure 2, where it can be seen that the platoon phase occupies almost the entire low-density phase.

3.4. Kinetics of platoon formation

In the infinite or periodic system an initially homogeneous configuration with density $\rho < \rho^*$ approaches the phase-separated state through a coarsening process, characterized by a power law increase of the typical size $\xi(t)$ of platoons or gaps between platoons. Based on the analogy

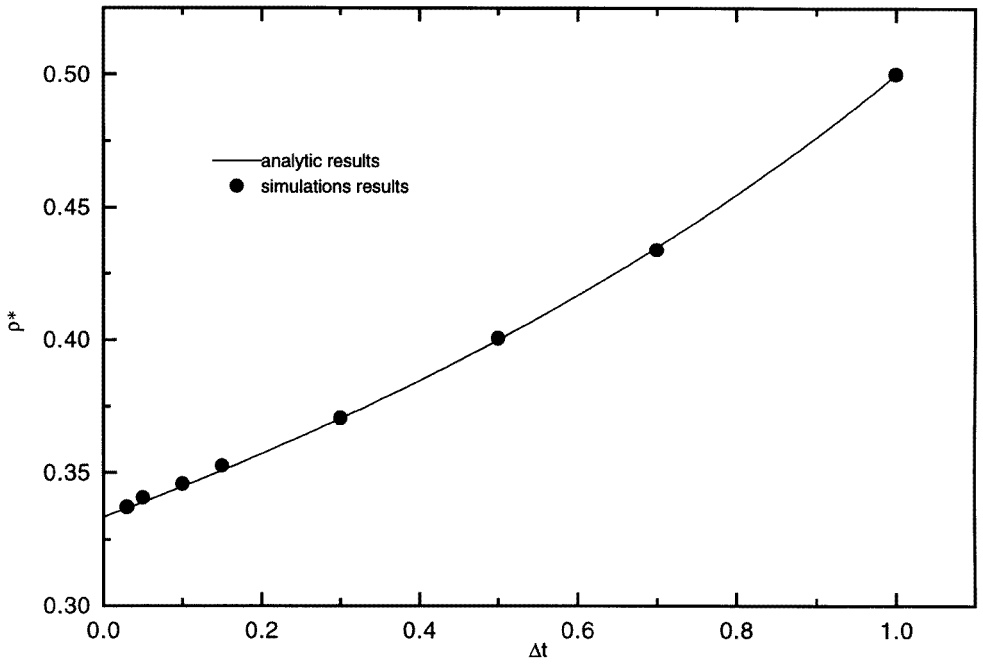

Figure 6. The variation of the critical density ρ^*, for platoon formation as a function of Δt for $L = 2000$, $n = 1$ and $c = \frac{1}{2}$. The full curve denotes the analytical result (10). The points denote the numerical data.

with a deterministic model of platoon formation [7], this power law was conjectured [9] to be given by

$$\xi(t) \sim t^{(n+1)/(n+2)} \tag{11}$$

where the exponent n characterizes the behaviour of the probability distribution of jump rates $f(p)$ (see equation (4)). The fact that $\xi(t)$ grows sublinearly with time, i.e. $\lim_{t\to\infty} \xi(t)/t = 0$, can be proved rigorously [23].

Numerical tests of the prediction (11) were performed for the periodic system with random sequential ($\Delta t \to 0$) [9] and fully parallel ($\Delta t \to 1$) [19] dynamics. In [9] deviations from the power law (11) were detected, while full agreement with (11) was found in [19]. Since different measures of the platoon size were used in the two studies, a direct comparison is difficult [18].

We have therefore readdressed the issue within our model, which allows continuous interpolation between fully parallel and random sequential dynamics. Figure 7 shows numerical data for the variance of particle headways $\Delta^2(t)$ which, under mild assumptions [18], can be shown to be proportional to $\xi(t)$, for large systems ($L = 10^5$) with various values of Δt and both periodic and open boundary conditions. For systems of this size the boundary conditions are not expected to matter on the timescales of interest. All the data are in reasonable agreement with the relation (11), which predicts $\xi \sim t^{2/3}$ in our case. We attribute the slight decrease of the exponent at long times to the onset of boundary effects.

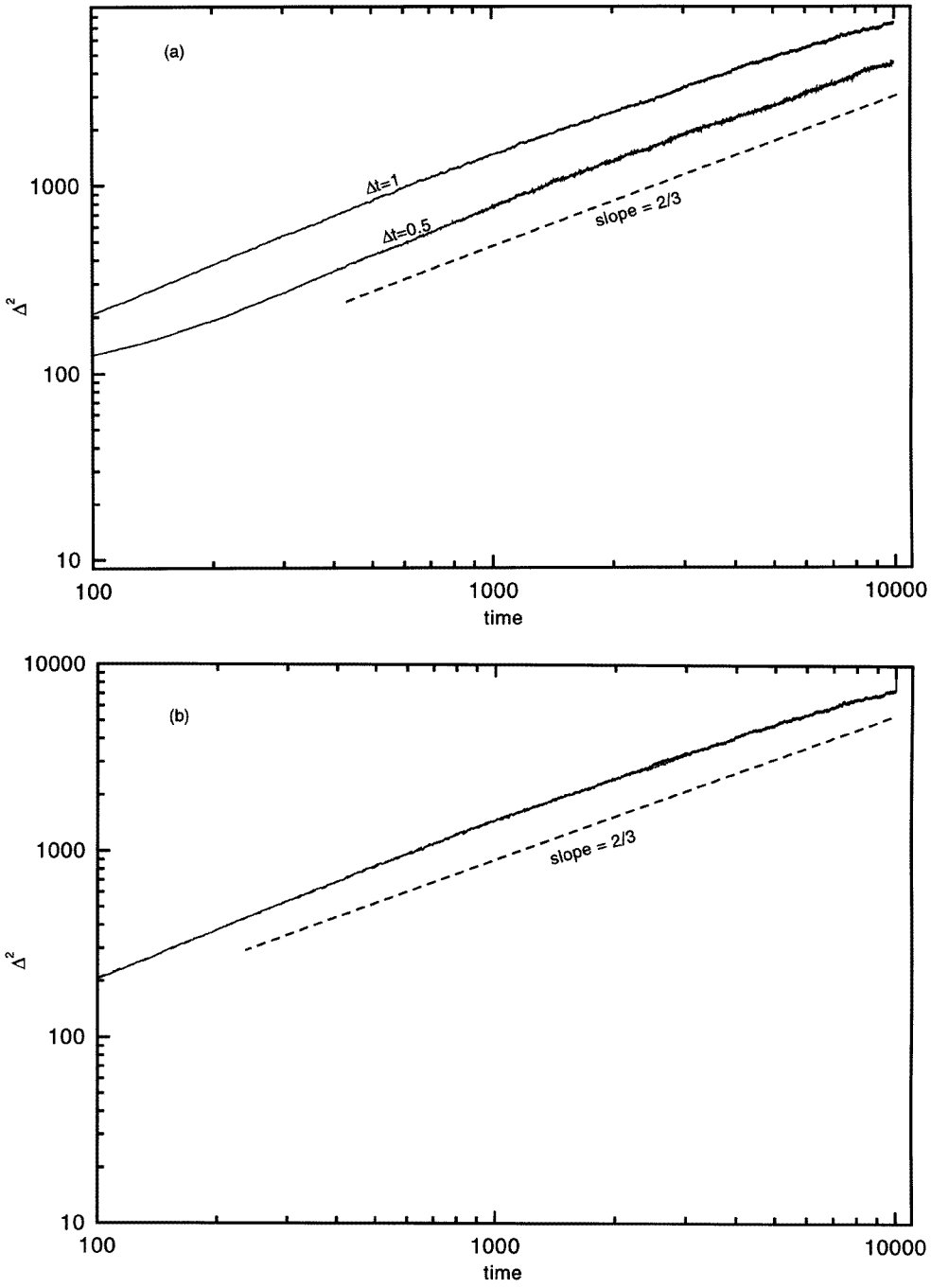

Figure 7. Time dependence of the headway variance Δ^2, for $L = 10^5$, $n = 1$ and $c = \frac{1}{3}$. (*a*) Open boundary conditions with $\alpha = 0.28$ and $\beta = 0.6$. (*b*) Parallel update for $\Delta t = 1$. The curve is a juxtaposition of simulations data obtained with a periodic boundary conditions with $\rho = \frac{1}{3}$ and open boundary conditions with $\alpha = 0.28$ and $\beta = 0.6$.

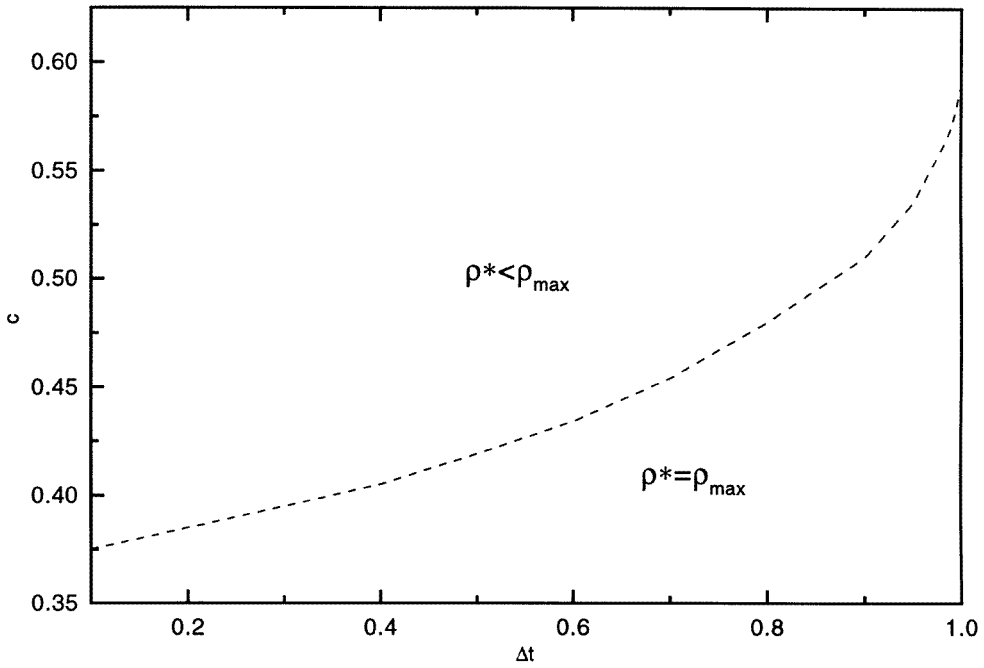

Figure 8. Phase diagram in the $(c, \Delta t)$-plane for $n = 2$. The broken curve separate two regions: $\rho^* < \rho_{\max}$ and $\rho^* = \rho_{\max}$.

3.5. The case $\rho^* = \rho_{max}$

All the results presented so far were obtained for $n = 1$ in (4), which belongs to the regime of second-order platoon phase transitions in the sense of [9]. In this regime the derivative of the current $J(\rho)$, or, equivalently, of the velocity $v(\rho) = J(\rho)/\rho$, with respect to ρ is continuous at $\rho = \rho^*$. Consequently the current–density relation has the qualitative shape shown in figure 3, with a quadratic maximum at a density $\rho_{\max}$ strictly larger than ρ^*. On the other hand, for $n > 1$ the platoon transition becomes first order, and it is possible to choose parameters such that the critical density ρ^* coincides with the maximum-current density $\rho_{\max}$. In figure 8 the corresponding region in the $(c, \Delta t)$-plane is shown for $n = 2$, as computed analytically from equation (6). Below the dashed line in figure 8, where $\rho^* = \rho_{\max}$, the current–density relation displays a cusp at the maximum (figure 9).

The mean-field theory of boundary-induced phase transitions [3, 24] shows that the characteristics of such transitions depend crucially on the behaviour of $J(\rho)$ near its maximum. For example, if

$$J(\rho_{\max}) - J(\rho) \sim |\rho - \rho_{\max}|^m \tag{12}$$

then the density profile in the maximum-current phase decays, within the mean field, as $\rho(x) \sim x^{1/(m-1)}$. In the generic case $m = 2$ fluctuations change the power law to $\rho(x) \sim 1/\sqrt{x}$ [3, 13, 14, 16, 25], while for $m = 4$ the fluctuations were argued [3] to be irrelevant. The only exactly solved case with $m \neq 2$ is the deterministic limit $p_\mu \equiv 1$ of the fully parallel TASEP, for which $m = 1$ and it is found [21] that the maximum-current phase disappears altogether.

In the disordered model the current–density relation can be changed from $m = 2$ to $m = 1$ by the choice of n, c and Δt. It therefore seemed worthwhile to obtain the (α, β)-phase diagram also for a parameter set below the dotted line in figure 8, corresponding to $m = 1$. The

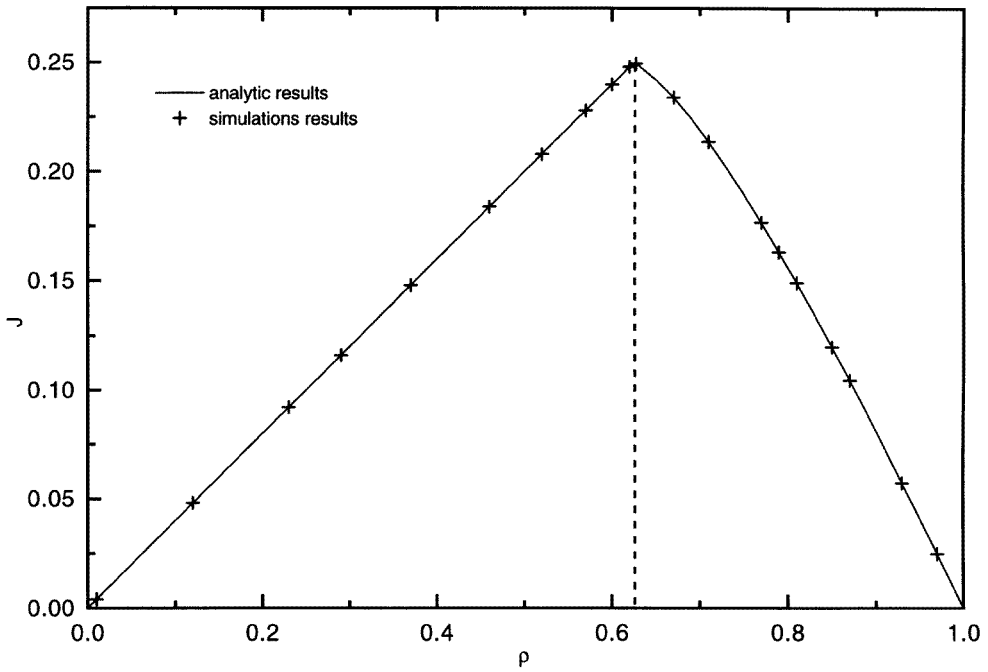

Figure 9. The variation of the current J as a function of density ρ for $L = 2000$, $\Delta t = 1$, $n = 2$ and $c = 0.4$. The vertical dotted line represents the critical density ($\rho = \rho^* = \rho_{\max}$)

method used for the computation was described above in section 3.1. The result is shown in figure 10. The topology of the phase diagram is similar to the other cases (see figure 2), and the maximum-current phase is seen to persist. The density profile in the maximum-current phase is shown in figure 11. While the data are too noisy to precisely determine the decay exponent, they are certainly consistent with a $1/\sqrt{x}$-decay, as in the pure case [3, 13, 14, 16, 25]; a fit in the range $1 \leqslant i \leqslant 300$ yields an exponent of 0.47 ± 0.06. Thus, in contrast to mean-field theory [3], the density profile appears to be insensitive to the order of the current maximum.

4. Conclusions

Using numerical simulations, we have studied the effect of particlewise disorder on the phase diagram for the asymmetric exclusion model with open boundaries and a hopping rate parameter Δt, which interpolates between random sequential and fully parallel dynamics. Apart from effects of the broken particle–hole symmetry, such as the (slight) shift of the first-order transition line away from the line $\alpha = \beta$, the phase diagram was found to be rather similar to that obtained in the pure case [13, 14, 16]. One explanation for the fact that the effects of disorder are, perhaps, less pronounced than expected, was indicated in section 3.3. Since the lifetime of particles within the open system is only of the order L, there is no time for the disorder-induced density inhomogeneities (platoons) to develop up to the scale of the system size; using (11) one estimates that they reach a size of the order $L^{(n+1)/(n+2)}$, which is small compared with L when $L \to \infty$ for any n.

On the other hand, we have seen that the platoon phase transition occurring in the low-density phase retains most of the features observed previously in systems with periodic

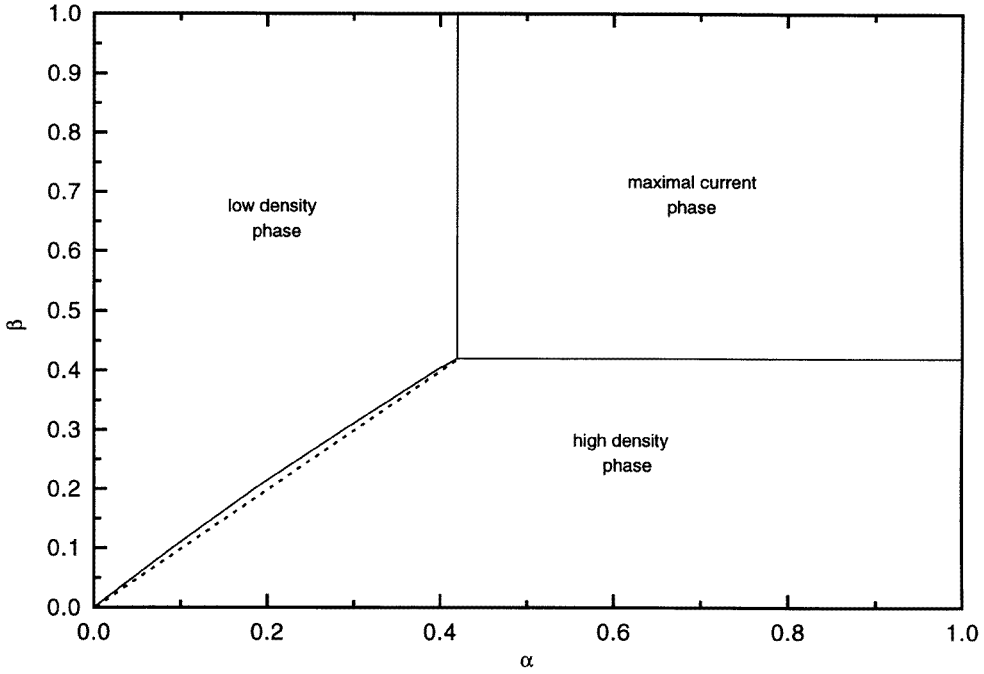

Figure 10. Phase diagram in the (α, β)-plane for $L = 2000$, $\Delta t = 1$, $n = 2$ and $c = 0.4$. The dotted line represents the line $\alpha = \beta$.

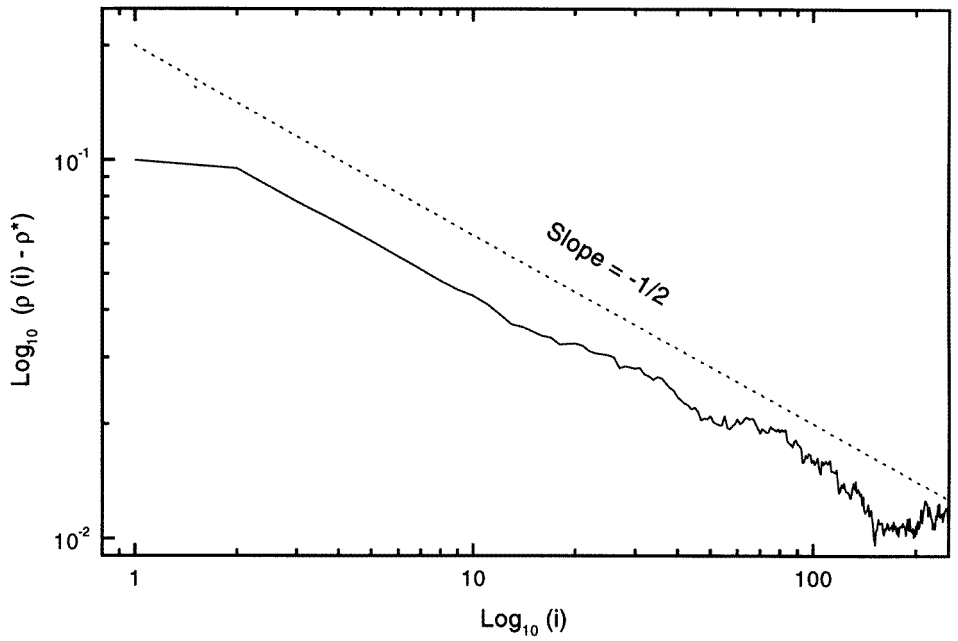

Figure 11. A double-logarithmic plot of the density profile for $L = 1000$, $\Delta t = 1$, $c = 0.4$, $n = 2$, $\alpha = 0.9$ and $\beta = 0.7$. The dotted line indicates the $1/\sqrt{x}$-decay expected for the pure system.

boundary conditions, and the analytic results obtained for this case [9, 10, 17] were also quantitatively confirmed for the open system. Surprisingly, we found that a disorder-induced cusp at the maximum of the current–density relation changes neither the topology of the phase diagram, nor the decay of the density profile in the maximum-current phase. The consequences of such singularities on boundary-induced phase transitions should be explored in future work.

Acknowledgments

JK wishes to thank the Faculté des Sciences, Rabat, for the warm hospitality shown during a visit when this work was initiated, and G Schütz for a useful discussion. He also acknowledges the support of DFG within SFB 237 *Unordnung und grosse Fluktuationen*. We are indebted to an anonymous referee for asking a helpful question.

References

[1] Schütz G 1997 *Int. J. Mod. Phys.* B **11** 197 and references therein
[2] Nagel K 1996 *Phys. Rev.* E **53** 4655
[3] Krug J 1991 *Phys. Rev. Lett.* **67** 1882
[4] Janowsky S A and Lebowitz J L 1992 *Phys. Rev.* A **45** 618
[5] Csahok Z and Vicsek T 1994 *J. Phys. A: Math. Gen.* **27** L591
[6] Tripathy G and Barma M 1998 *Phys. Rev.* E **58** 1911
[7] Ben-Naim E, Krapivsky P and Redner S 1994 *Phys. Rev.* E **50** 822
[8] Benjamini I, Ferrari P A and Landim C 1996 *Stoch. Process. Appl.* **61** 181
[9] Krug J and Ferrari P A 1996 *J. Phys. A: Math. Gen.* **29** L465
[10] Evans M R 1996 *Europhys. Lett.* **36** 13
[11] Mallick K 1996 *J. Phys. A: Math. Gen.* **29** 5375
[12] Newell G F 1959 *Opns. Res.* **7** 589
[13] Schütz G and Domany E 1993 *J. Stat. Phys.* **72** 277
[14] Derrida B, Evans M R, Hakim V and Pasquier V 1993 *J. Phys. A: Math. Gen.* **26** 1493
[15] Rajewsky N, Santen L, Schadschneider A and Schreckenberg M 1998 *J. Stat. Phys.* **92** 151
[16] Evans M R, Rajewsky N and Speer E R 1998 *Preprint* cond-mat/9810306 *J. Stat. Phys.* to appear (April 1999)
[17] Evans M R 1997 *J. Phys. A: Math. Gen.* **30** 5669
[18] Krug J 1998 *Traffic and Granular Flow '97* ed M Schreckenberg and D E Wolf (Singapore: Spinger) p 285
[19] Ktitarev D V, Chowdhury D and Wolf D E 1997 *J. Phys. A: Math. Gen.* **30** L221
[20] Benyoussef A, Chakib H and Ez-Zahraouy H 1999 *Eur. Phys. J.* B to appear
[21] Tilstra L G and Ernst M H 1998 *J. Phys. A: Math. Gen.* **31** 5033
[22] Krug J and Tang L-H 1994 *Phys. Rev.* E **50** 104
[23] Seppäläinen T and Krug J 1999 *J. Stat. Phys.* to appear (May 1999)
[24] Krug J 1991 *Spontaneous Formation of Space–Time Structures and Criticality* ed T Riste and D Sherrington (Dordrecht: Kluwer) p 37
[25] Janssen H K and Oerding K 1996 *Phys. Rev.* E **53** 4544